PERGAMON

International Journal of Heat and Mass Transfer 43 (2000) 3093–3104

International Journal of HEAT and MASS TRANSFER

www.elsevier.com/locate/ijhmt

Forced convection from a rotationally oscillating cylinder placed in a uniform stream

F.M. Mahfouz, H.M. Badr*

Mechanical Engineering Department, King Fahd University of Petroleum and Minerals, Dhahran, Saudi Arabia

Received 31 December 1998; received in revised form 27 October 1999

Abstract

Forced convection from a heated cylinder performing rotational oscillation about its own axis and placed in a uniform stream is investigated. The governing equations of motion and energy are solved numerically to determine the flow field characteristics and the heat transfer coefficients. The main dominating parameters are Reynolds numbers, Re, Prandtl number, Pr, amplitude of oscillation, Θ_A, and the frequency ratio, F_R, which represents the ratio between the frequency of oscillation, f, and the natural frequency of vortex shedding, f_0. The ranges considered for these parameters are $40 \leq Re \leq 200$, $0 \leq \Theta_A \leq \pi$ and $0 \leq F_R \leq 2$, while the Prandtl number is kept constant at 0.7. The lock-on phenomenon has been detected and its effect on the thermal field has been determined. The results show that the lock-on phenomenon occurs within a band of frequency near the natural frequency and the heat transfer coefficient has shown appreciable increase in the lock-on frequency range.

Keywords: Convection; Cylinder; Oscillations; Rotation; Vortex shedding; Lock-on

1. Introduction

The circular cylinder has long inspired researchers as a successful model for studying important aspects of heat transfer and hydrodynamics associated with unsteady flows over bluff bodies. In the case of flow past stationary cylinder, as Reynolds number exceeds about 40, alternating vortices are shed periodically and arranged downstream in a Karman vortex street. This vortex shedding process is found to cause unsteady flow behavior near the cylinder surface and in turn enhance heat transfer. This heat transfer enhancement under natural shedding process has stimulated the interest of researchers to study the potential of enhancing heat convection using various forms of unsteady excitations. Among these is the use of forced oscillations.

When a cylinder performs rectilinear oscillations at a frequency close to the natural shedding frequency in the case of transverse oscillations or twice the natural shedding frequency in the case of in-line oscillations, vortices start shedding at the same forcing frequency. In the case of rotational oscillations, vortices are shed at the same forcing frequency only when the frequency is within a range bracketing the natural shedding frequency. This is called the lock-on phenomenon and is reported for rectilinear oscillation in the works of Tanida et al. [1], Bishop and Hassan [2], Hurlbut et al. [3], Stansby [4] and Griffin and Ramberg [5].

The lock-on phenomenon in the case of a cylinder performing rotational oscillations in a cross stream

* Corresponding author.

0017-9310/00/$ - see front matter
PII: S0017-9310(99)00326-9

was reported by only few investigators. Okajima et al. [6] was the first to report this phenomenon when he investigated the problem theoretically in the range of Re from 40 to 80 and experimentally in the range from 80 to 6100. Tokumaru et al. [7] also reported the lock-on phenomenon in his experimental study of rotary oscillation control of a cylinder wake at $Re = 15{,}000$. Lu and Sato [8] reported the phenomenon when they investigated numerically the same problem mainly at $Re = 1000$ while Chou [9] reported it at $Re = 500$, 1000. The other authors who investigated the same problem did not report this phenomenon because of either using the boundary-layer assumption, as in the work by Hori [10], or utilizing a range of frequency far away from the natural shedding frequency, as in the work by Tanida [11]. Flow over a rotationally oscillating cylinder was also investigated by Wu et al. [12] at frequencies equal or near the natural shedding frequency. The study has shown that a resonant flow state was achieved with lift and drag components reaching their maximum. Moreover, Tokumaru et al. [13] investigated the lift variation when a cylinder executes rotary oscillation with net rate of rotation, whereas, Filler et al. [14] investigated the frequency response of the shear layers separating from a cylinder performing rotational oscillations with small amplitudes.

Experimental investigation of the problem of forced convection from a cylinder performing in-line or transverse oscillations was carried out by several researchers. In the case of in-line oscillation, Zijnen [15] observed a decrease in the heat transfer for low Reynolds number flows ($Re < 5$), while Leung et al. [16] found that for $Re < 15{,}000$ the heat transfer rates may be enhanced as either the frequency or amplitude of oscillation is increased. Takahashi and Endoh [17] investigated the same problem experimentally and observed an increase in heat transfer provided that the velocity amplitude was above a certain limit. However, for the case of transverse oscillations, conflicting results were obtained by several authors. For example, Kezios and Prasanna [18] reported about 20% increase in heat transfer rates, while the experimental study by Sreenivasan and Ramashandran [19] showed no appreciable increase in heat transfer. On the other hand, Saxena and Laird [20] reported significant increase in heat rates at $Re = 3500$ which was found to be coincident with larger flow disturbances that result when the frequency and amplitude of oscillation tend to force eddies to lock-on to the cylinder oscillation. In their work, Chin-Hsiang et al. [21] reported a maximum of 34% increase in heat transfer within the range of parameters considered in their experiments. They attributed this increase to the lock-on phenomenon.

The first theoretical study of forced convection from an oscillating cylinder was reported by Karanth et al. [22] who obtained numerical solutions for both cases of in-line and transverse oscillations. However, in their calculation, the Reynolds number is fixed at 200 and the cylinder is considered to oscillate exactly at a fixed lock-on frequency which perhaps explains the increase in heat rates that they have reported for both types of oscillation. A more thorough investigation of the effect of the lock-on phenomenon on heat transfer was reported by Cheng et al. [23]. Within the lock-on frequency range, they found an appreciable increase in heat transfer, however, outside that range, the heat transfer was almost unaffected by oscillations. A correlation expressing the dependence of heat transfer on the dominant parameters in the lock-on regime was presented.

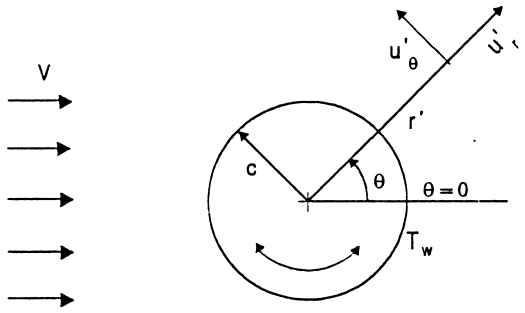

Fig. 1. Coordinate system.

Based on the above literature search, it is clear that several investigators focused on the effect of rectilinear oscillations on heat transfer, while little attention was given to the effect of rotational oscillations. The only theoretical study on the effect of rotational oscillations was carried out by Childs and Mayle [24]. The study was based on boundary-layer simplifications and limited to very small amplitudes. The results showed no enhancement in heat transfer which was attributed to the aforementioned assumptions. The main objective of this work is to study the effect of rotational oscillation on the local and the time-average heat transfer from a cylinder placed in a cross stream with emphasis on the lock-on phenomenon. The flow is assumed to be laminar and two-dimensional, and the oscillations are only harmonic.

2. Problem statement and formulation

Fig. 1 shows the physical model where a cylinder of radius c is placed horizontally in an unbounded, cross-stream with uniform approaching velocity V. The cylinder surface is maintained at a constant temperature T_w and is rotationally oscillating about its own axis with harmonic motion of the form:

$$\Theta = -\Theta_A \cos(2\pi f\tau) \tag{1}$$

where Θ is the angular displacement and τ is the time. Θ_A and f are the angular amplitude and frequency of oscillation, respectively. The conservation equations that govern the laminar, two-dimensional motion of incompressible fluid are the continuity and momentum equations. The analysis of heat convection is based on the two-dimensional unsteady energy conservation principle. In cylindrical coordinates, the governing equations in the stream function-vorticity form are expressed as:

$$\frac{\partial\zeta'}{\partial\tau} + \frac{\partial\psi'}{r'\partial\theta}\frac{\partial\zeta'}{\partial r'} - \frac{\partial\psi'}{r'\partial r'}\frac{\partial\zeta'}{\partial\theta} = \nu\nabla^2\zeta' \tag{2}$$

$$\zeta' = -\nabla^2\psi' \tag{3}$$

$$\frac{\partial T}{\partial\tau} + \frac{\partial\psi'}{r'\partial\theta}\frac{\partial T}{\partial r'} - \frac{\partial\psi'}{\partial\theta}\frac{\partial T}{r'\partial\theta} = \frac{k}{\rho c_p}\nabla^2 T \tag{4}$$

where T is the fluid temperature, ψ' is the stream function and ζ' is the vorticity defined as

$$\zeta' = \left(\frac{\partial u'_\theta}{\partial r'} + \frac{u'_\theta}{r'} - \frac{\partial u'_r}{r'\partial\theta}\right)$$

The boundary conditions to be satisfied are the no-slip, impermeability and isothermal conditions on the cylinder surface together with the free stream conditions far away. These conditions can be expressed as

$$\psi' = \frac{\partial\psi'}{\partial\theta} = 0, \quad \frac{\partial\psi'}{\partial r'} = -u'_w, \quad \text{and} \quad T = T_w \quad \text{at } r' = c,$$

$$\frac{\partial\psi'}{\partial\theta} \to r'V\cos\theta, \quad \frac{\partial\psi'}{\partial r'} \to -V\sin\theta, \quad \zeta' \to 0 \quad \text{and} \quad T \to T_\infty \quad \text{as } r' \to \infty \tag{5}$$

The dimensionless forms of the above equations are obtained by introducing the following dimensionless quantities.

$$r = \frac{r'}{c}, \quad t = \tau\frac{V}{c}, \quad \psi = \frac{\psi'}{cV}, \quad \zeta = -\zeta'\frac{c}{V}, \quad \text{and} \quad \phi = (T - T_\infty)/(T_s - T_\infty)$$

Using the above transformation and introducing the modified polar coordinates (ξ, θ) where $\xi = \ln r$, the equations can be written as:

$$e^{2\xi}\frac{\partial\zeta}{\partial t} = \frac{2}{Re}\left(\frac{\partial^2\zeta}{\partial\xi^2} + \frac{\partial^2\zeta}{\partial\theta^2}\right) - \frac{\partial\psi}{\partial\theta}\frac{\partial\zeta}{\partial\xi} + \frac{\partial\psi}{\partial\xi}\frac{\partial\zeta}{\partial\theta} \tag{6}$$

$$e^{2\xi}\zeta = \frac{\partial^2\psi}{\partial\xi^2} + \frac{\partial^2\psi}{\partial\theta^2} \tag{7}$$

$$e^{2\xi}\frac{\partial\phi}{\partial t} = \frac{2}{Re\,Pr}\left(\frac{\partial^2\phi}{\partial\xi^2} + \frac{\partial^2\phi}{\partial\theta^2}\right) - \frac{\partial\psi}{\partial\theta}\frac{\partial\phi}{\partial\xi} + \frac{\partial\psi}{\partial\xi}\frac{\partial\phi}{\partial\theta} \tag{8}$$

where $Re = 2cV/\nu$ is the Reynolds number and $Pr = \mu c_p/k$ is the Prandtl number. The cylinder surface dimensionless velocity can be expressed as

$$U_w = \alpha\sin(\pi St) \tag{9}$$

where α represents the velocity amplitude of oscillation and S is the dimensionless forcing frequency $(= 2cf/V)$. The dimensionless form of the boundary conditions given in Eq. (5) can be expressed as:

$$\psi = \frac{\partial\psi}{\partial\theta} = 0, \quad \frac{\partial\psi}{\partial\xi} = -\alpha\sin(\pi St), \quad \text{and} \quad \phi = 1 \quad \text{at } \xi = 0,$$

$$\frac{\partial\psi}{\partial\theta} \to e^{-\xi}\cos\theta, \quad \frac{\partial\psi}{\partial\xi} \to -e^{-\xi}\sin\theta, \quad \zeta \to 0 \quad \text{and} \quad \phi \to 0 \quad \text{as } \xi \to \infty \tag{10}$$

3. The method of solution

The method of solution is based on integrating the governing equations of motion and energy in time to obtain the velocity and temperature fields. Using the series truncation method and following the works of Collins and Dennis [25] and Badr and Dennis [26], the dimensionless stream function ψ, vorticity ζ and temperature ϕ are approximated using Fourier series expansions as follows:

$$\psi(\xi,\theta,t) = \frac{1}{2}F_0(\xi,t) + \sum_{n=1}^{N}\left[f_n(\xi,t)\sin(n\theta) + F_n(\xi,t)\cos(n\theta)\right],$$

$$\zeta(\xi,\theta,t) = \frac{1}{2}G_0(\xi,t) + \sum_{n=1}^{N}\left[g_n(\xi,t)\sin(n\theta) + G_n(\xi,t)\cos(n\theta)\right]$$

$$\phi(\xi,\theta,t)=\frac{1}{2}H_0(\xi,t)+\sum_{n=1}^{N}\left[h_n(\xi,t)\sin(n\theta)+H_n(\xi,t)\cos(n\theta)\right] \tag{11}$$

where F_0, f_n, F_n, G_0, g_n, G_n, H_0, h_n, and H_n are the Fourier coefficients and N represents the order of truncation. Substitution of Eq. (11) into Eqs. (3) and (4) and using simple mathematical analysis results in the following set of differential equations:

$$\frac{\partial^2 F_0}{\partial\xi^2}=e^{2\xi}G_0 \tag{12a}$$

$$\frac{\partial^2 f_n}{\partial\xi^2}-n^2 f_n=e^{2\xi}g_n \tag{12b}$$

$$\frac{\partial^2 F_n}{\partial\xi^2}-n^2 F_n=e^{2\xi}G_n \tag{12c}$$

$$e^{2\xi}\frac{\partial G_0}{\partial t}=\frac{2}{Re}\frac{\partial^2 G_0}{\partial\xi^2}+S_0 \tag{13a}$$

$$e^{2\xi}\frac{\partial g_n}{\partial t}=\frac{2}{Re}\left(\frac{\partial^2 g_n}{\partial\xi^2}-n^2 g_n\right)+nF_n\frac{\partial G_0}{\partial\xi}-nG_n\frac{\partial F_0}{\partial\xi}+S_{n1} \tag{13b}$$

$$e^{2\xi}\frac{\partial G_n}{\partial t}=\frac{2}{Re}\left(\frac{\partial^2 G_n}{\partial\xi^2}-n^2 G_n\right)+nf_n\frac{\partial G_0}{\partial\xi}-ng_n\frac{\partial F_0}{\partial\xi}+S_{n2} \tag{13c}$$

$$e^{2\xi}\frac{\partial H_0}{\partial t}=\frac{2}{Re\,Pr}\frac{\partial^2 H_0}{\partial\xi^2}+Z_0 \tag{14a}$$

$$e^{2\xi}\frac{\partial h_n}{\partial t}=\frac{2}{Re\,Pr}\left(\frac{\partial^2 h_n}{\partial\xi^2}-n^2 h_n\right)+nF_n\frac{\partial H_0}{\partial\xi}-nH_n\frac{\partial F_0}{\partial\xi}+Z_{n1} \tag{14b}$$

$$e^{2\xi}\frac{\partial H_n}{\partial t}=\frac{2}{Re\,Pr}\left(\frac{\partial^2 H_n}{\partial\xi^2}-n^2 H_n\right)+nf_n\frac{\partial H_0}{\partial\xi}-nh_n\frac{\partial F_0}{\partial\xi}+Z_{n2} \tag{14c}$$

where S_0, S_{n1}, S_{n2}, Z_0, Z_{n1} and Z_{n2} are all easily identifiable functions of ξ and t. Eqs. (12a)–(12c) define a set of $(2N+1)$ ordinary differential equations and each of Eqs. (13) and (14) define another set of $(2N+1)$ partial differential equations. All these equations $(6N+3)$ have to be solved at every time step to get the details of the flow and thermal fields. The boundary conditions for all functions present in Eqs. (12)–(14) are obtained from Eqs. (10) and can be expressed as

$$F_0=F_n=f_n=\partial F_n/\partial\xi=\partial f_n/\partial\xi=0,$$

$$\partial F_0/\partial\xi=-2\alpha\sin(\pi St),$$

$$H_0=2,\ H_n=h_n=0 \quad \text{at } \xi=0, \tag{15a}$$

and

$$F_0,\ \partial F_0/\partial\xi,\ F_n,\ \partial F_n/\partial\xi\to 0,\quad f_n\to\delta_{1,n},$$

$$e^{-\xi}\partial f_n/\partial\xi\to\delta_{1,n},$$

$$G_0,\ G_n,\ g_n\to 0,\ \text{and } H_0,\ H_n,\ h_n\to 0 \quad \text{as } \xi\to\infty \tag{15b}$$

Integrating both sides of Eq. (12a) with respect to ξ between $\xi=0$ and ∞ and using the boundary conditions in Eq. (15) gives the following integral condition:

$$\int_0^\infty e^{2\xi}G_0\,d\xi=2\alpha\sin(\pi St) \tag{16a}$$

Integrating both sides of Eqs. (12b) and (12c) after multiplying by $e^{-n\xi}$ and making use of the boundary conditions (15), one can obtain the following integral conditions

$$\int_0^\infty e^{(2-n)\xi}g_n\,d\xi=2\delta_{1,n} \tag{16b}$$

$$\int_0^\infty e^{(2-n)\xi}G_n\,d\xi=0 \tag{16c}$$

where

$$\delta_{1,n}=\begin{cases}1 & \text{when } n=1\\ 0 & \text{when } n\neq 1\end{cases}$$

The above integral conditions are used at every time step to calculate the values of the functions G_0, g_n and G_n on the cylinder surface ($\xi=0$). These functions are then used to compute accurately the vorticity distribution on the cylinder surface. The first condition (16a) is essential to ensure the periodicity of the pressure on the surface.

In this study, it is assumed that the flow and the imposed rotational oscillatory motion start simul-

taneously and impulsively from rest. The cylinder surface temperature is assumed as well to increase suddenly to T_w. The flow field structure at small times following the impulsive fluid motion is characterized by a very thin boundary-layer region close to the cylinder surface bounded by a potential flow elsewhere. For proper scaling at small time, we use the boundary-layer coordinates (z, t) defined as $\xi = \lambda z$, where $\lambda = 2\sqrt{2t/Re}$.

Now, by introducing $\psi^* = \psi/\lambda$, and $\zeta^* = \lambda\zeta$ and closely following the methodology of Collins and Dennis [25] and Badr and Dennis [26], the initial solutions at $t = 0^+$ are found to be

$$\psi^*(z, \theta, 0) = -2\Big[z\big(1-\mathrm{erf}(z)\big)+\pi^{-1/2} \times \big(1-\mathrm{e}^{-z^2}\big)\Big]\sin(\theta) \tag{17}$$

$$\zeta^*(z, \theta, 0) = 4\pi^{-1/2}\mathrm{e}^{-z^2}\sin(\theta) \tag{18}$$

$$\phi(z, 0) = -\mathrm{erf}\big(z\sqrt{Pr}\big) + 1 \tag{19}$$

Eq. (19) allows starting the integration of the energy equation to be carried out simultaneously with the flow equations starting from $t = 0$.

The local and average Nusselt numbers are defined as

$$Nu = \frac{hd}{k}, \quad \overline{Nu} = \frac{\bar{h}d}{k} \tag{20}$$

where, h and $\bar{h}$ are the local and average heat transfer coefficients which are defined as

$$h = \frac{q'}{T_w - T_\infty}, \quad \bar{h} = \frac{1}{2\pi}\int_0^{2\pi} h \, \mathrm{d}\theta$$

where q' is heat transfer rate given by $q' = -k\frac{\partial T}{\partial r'}|_{r'=c}$. From the above definitions and using Eq. (11), one can deduce

$$Nu = -2\left(\frac{\partial\phi}{\partial\xi}\right)_{\xi=0} = -\left\{\frac{\partial H_0}{\partial\xi} + 2\sum_{n=1}^{N}\left[\frac{\partial h_n}{\partial\xi}\sin(n\theta) + \frac{\partial H_n}{\partial\xi}\cos(n\theta)\right]\right\}_{\xi=0} \tag{21}$$

and

$$\overline{Nu} = -\left(\frac{\partial H_0}{\partial\xi}\right)_{\xi=0} \tag{22}$$

The time-averaged Nusselt number is obtained from

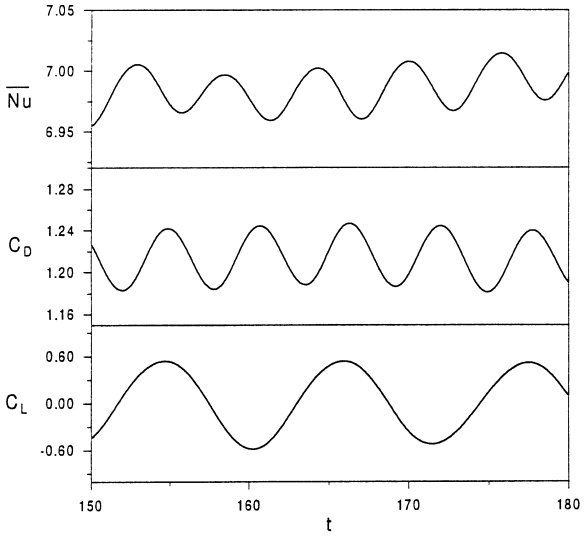

Fig. 2. Time variation of C_D, C_L and $\overline{N}$ in the case of a fixed cylinder at $Re = 200$.

$$\overline{\overline{Nu}} = \frac{1}{t_2 - t_1}\int_{t_1}^{t_2} \overline{Nu} \, \mathrm{d}t \tag{23}$$

where the time period between t_1 and t_2 is taken after reaching the quasi-steady state and covering more than one cycle. The drag and lift coefficients can be expressed in terms of Fourier coefficients as

$$C_D = \frac{2\pi}{Re}\left\{g_1(0, t) - \left(\frac{\partial g_1}{\partial\xi}\right)_{\xi=0}\right\} \quad \text{and} \quad C_L = -\frac{2\pi}{Re}\left\{G_1(0, t) - \left(\frac{\partial G_1}{\partial\xi}\right)_{\xi=0}\right\} \tag{24}$$

The time variation of C_L is used to determine the frequency of vortex shedding.

4. Results and discussion

4.1. Accuracy of the method of solution

The case of flow over and heat transfer from a stationary cylinder was used to test the accuracy of the method of solution and the computational scheme. The phenomenon of vortex shedding was first examined at three Reynolds numbers. The dimensionless frequency of vortex shedding is normally expressed in terms of the natural Strouhal number, $S_0 = F_0 d/V$, where f_0 is the vortex shedding frequency. The predicted values of Strouhal number at Reynolds numbers $Re = 80$, 100 and 200 are shown in Table 1 together with the experimental measurements reported by Roshko [27] and Williamson [28]. The table also shows

Table 1
Predicted Strouhal number (S_0) and Nusselt number ($\overline{\overline{Nu}}$) for the case of fixed cylinder and comparison with previous studies

Re	S_0			$\overline{\overline{Nu}}$	
	Present study	Roshko [27]	Williamson [28]	Present study	Range of results [21,29–34]
80	0.156	0.155	0.153	4.80	4.59–4.95
100	0.16	0.165	0.164	5.31	4.769–5.52
200	0.18	0.18–0.2	0.183	6.99	6.67–7.8

the values of the time-averaged Nusselt number obtained from the present study for the case of forced convection together with the range of results reported in the literature by Chin-Hsiang et al. [21], Eckert and Soehngen [29], Kramers [30], Richardson [31], Morgan [32], Jain and Goel [33] and Rashid [34]. The present results lie approximately in the middle of the range of dispersed results reported by the other researchers. Fig. 2 shows the time variation of the average Nusselt number, $\overline{Nu}$, and the drag and lift coefficients, C_D and C_L, at $Re = 200$. While C_L oscillates with the same frequency of vortex shedding, C_D and $\overline{Nu}$ oscillate with twice of that frequency. This is mainly due to the nature of the vortex shedding mechanism in which vortices of opposite circulation shed alternately from the upper and lower sides of the cylinder surface. The period of C_D and $\overline{Nu}$ oscillations is the same as the time taken to detach one vortex, while the period of C_L oscillation is equal to the time taken to detach two vortices from the upper and lower sides of the surface. The incremental change in C_L is positive for one vortex and negative for the other because of the opposite circulation which is not the same for C_D and $\overline{Nu}$. The contour plots of isotherm patterns during one complete cycle of vortex shedding are shown in Fig. 3 for the case of $Re = 200$. It can be seen that the isotherm contours are very close near the cylinder surface and far apart away from it, which indicate large temperature gradients near the surface and small gradients far away.

Fig. 4 shows the variation of the local Nusselt number distribution over the surface during one complete cycle of vortex shedding for the same case ($Re = 200$). At all times, the maximum heat transfer rate is found near the front stagnation point $\theta = 180^\circ$. However, due to vortex shedding, the local heat transfer on the rear side of the cylinder improves, showing another local peak near $\theta = 360^\circ$. This local improvement in heat transfer increases the average heat transfer rate in comparison with the no vortex shedding solution. It can be also seen that the local Nusselt number distributions during one complete cycle are almost unchanged over most of the cylinder surface except on the rear part where remarkable differences are found as a result of periodic shedding of vortices. The local Nusselt number distributions at the beginning and at the end of the cycle confirm the cyclic behavior of the thermal field.

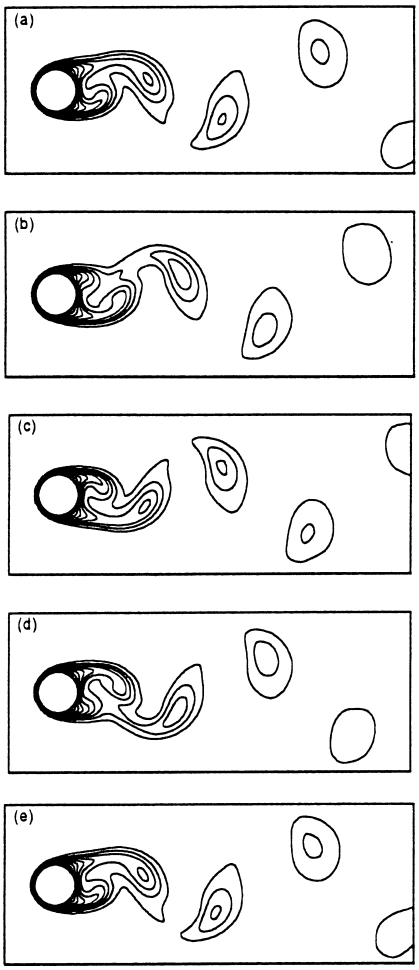

Fig. 3. Isotherm patterns in the case of a fixed cylinder at $Re = 200$; (a) $t = t_0$, (b) $t = t_0 + 2.75$, (c) $t = t_0 + 5.55$, (d) $t = t_0 + 8.25$, (e) $t = t_0 + T$, where $T = 11.1$ is the time period of a shedding cycle. The isotherms plotted are $\phi = 0.1(0.1)1.0$.

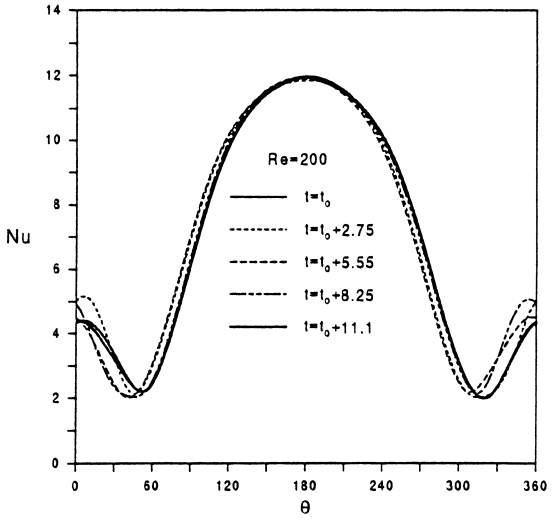

Fig. 4. Distribution of the local Nusselt number in a complete cycle of vortex shedding at $Re = 200$.

4.2. Effect of rotational oscillations

In the case of oscillating cylinder, the velocity and thermal fields are dominated by Reynolds number, Prandtl number, and the amplitude and frequency of oscillations. The study covers the range of Re up to 200, while the Prandtl number is kept constant at 0.7. The amplitude of oscillation, Θ_A, ranges between 0 and π and the oscillation frequency, S, ranges between 0 and $2S_0$, where S_0 is the natural Strouhal number.

The flow field in the wake region can be classified into lock-on and unlock-on regimes. The unlock-on regime is characterized by periodic shedding of vortices at natural frequency irrespective of the oscillation frequency. Such a regime occurs when the driving cylinder frequency, f, is either smaller or larger enough than the natural frequency, f_0. When the oscillation frequency approaches f_0, the lock-on regime occurs. In this regime, the vortices are shed at the forced frequency, i.e. the vortex shedding is synchronized with the cylinder oscillation. This is found to occur within a band of frequency that brackets the natural frequency and is called the range of synchronization or the lock-on frequency range. Fig. 5 shows a comparison between the lift records for lock-on and unlock-on regimes at $Re = 200$ and $\Theta_A = \pi/4$. For the unlock-on regime shown in Fig. 5(a), the lift force is fluctuating in wave forms, composed of two effects; one induced by the natural shedding and the other induced by the forced oscillations. In the lock-on regime shown in Fig. 5(b), the lift force is fluctuating with the forcing frequency only and with nearly uniform amplitude. Typical isotherm patterns for the unlock-on regime are shown in Fig. 6 for the case of $F_R = 0.5$, $Re = 200$ and

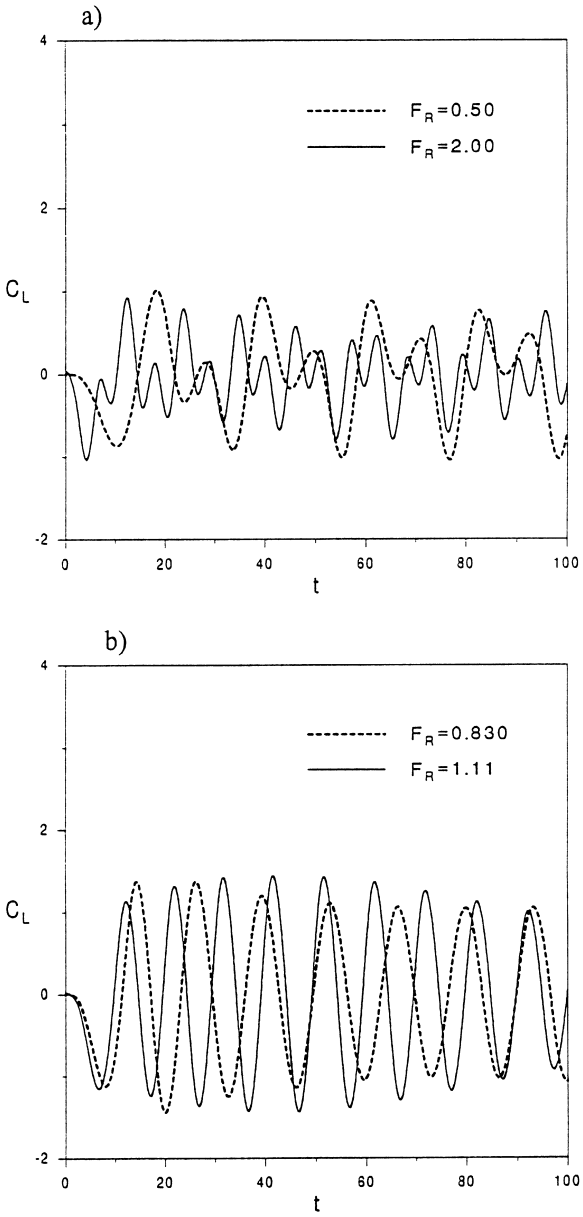

Fig. 5. The time variation of lift coefficient at $Re = 200$ and $\Theta_A = \pi/4$, (a) unlock-on regimes, (b) lock-on regimes.

$\Theta_A = \pi/4$. These patterns are prepared at almost equal intervals through one complete cycle. The figure shows that the thermal boundary layer is very thin near the forward stagnation point ($\Theta \sim 180^\circ$), and extends downstream to form an oscillating wake-shaped thermal layer. The figure also shows that the thermal wake, especially in the far wake region, is similar to that for a fixed cylinder. This feature characterizes, in general, the unlock-on regimes. Moreover, the two isotherm patterns at the beginning and end of the cycle

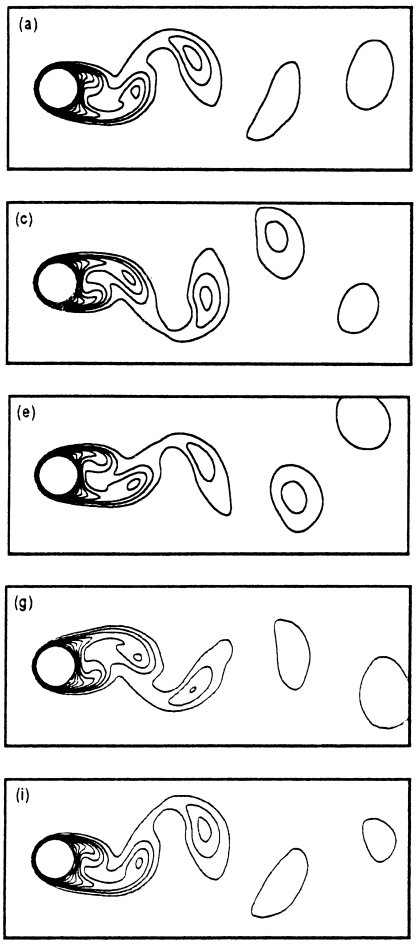

Fig. 6. Isotherm patterns in one complete cycle of unlock-on regime at $Re = 200$, $\Theta_A = \pi/4$ and $F_R = 0.5$; (a) $t = 40$, (c) $t = 45.5$, (e) $t = 51$, (g) $t = 56.5$ and (i) $t = 62$. The isotherms plotted are $\phi = 0.1(0.1)1.0$.

($t = 40$ and $t = 62$) are almost the same confirming the periodicity of the thermal field. Fig. 7 shows the distribution of the local Nusselt number at the same time intervals. Although the maximum and minimum values of Nu are almost the same at all times, the location clearly changes. However, the local Nusselt continues to have its lowest values at the rear part of the cylinder ($-60^\circ < \theta < 60^\circ$). The Nu distribution varies almost periodically with the cylinder oscillation. The time variation of the average Nusselt number at different frequencies below and above the lock-on range is shown in Fig. 8. The very high values of $\overline{Nu}$ at small time are due to the very small thermal boundary-layer thickness at the start of fluid motion. As time increases, the thermal boundary-layer thickness increases and $\overline{Nu}$ decreases but continues to fluctuate due to vortex shedding. It can be seen that $\overline{Nu}$ fluctuates with variant amplitude in a beating wave form.

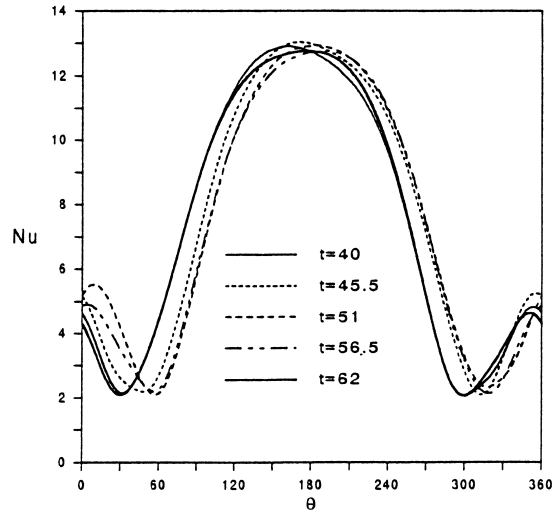

Fig. 7. The local Nusselt distribution in a complete cycle of unlock-on regime at $Re = 200$, $\Theta_A = \pi/4$ and $F_R = 0.5$.

Fig. 9 shows the time variation of average Nusselt number at different frequencies in the lock-on range for the case of $Re = 200$ and $\Theta_A = \pi/2$. It is clear from the figure that $\overline{Nu}$ fluctuates almost regularly with a frequency equal to twice the imposed cylinder frequency. The figure also shows an appreciable enhancement in heat transfer for high frequencies within the lock-on range. On the other hand, at low lock-on frequencies, the average Nusselt number becomes even smaller than that for a fixed cylinder (see, for example, the case of $F_R = 0.83$).

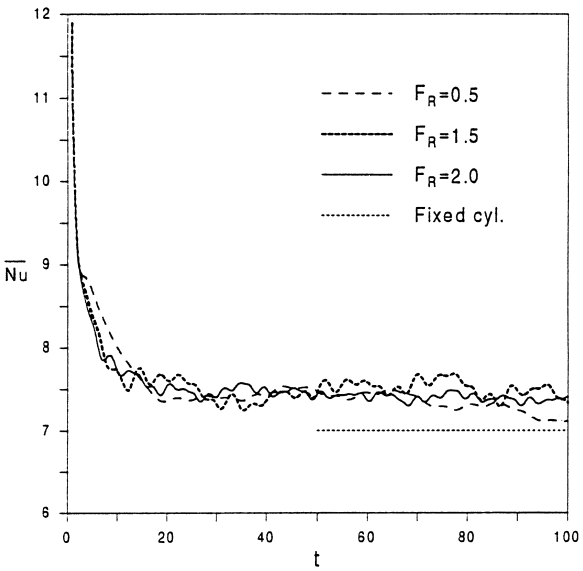

Fig. 8. The time variation of the average Nusselt number for unlock-on regimes at $Re = 200$ and $\Theta_A = \pi/4$.

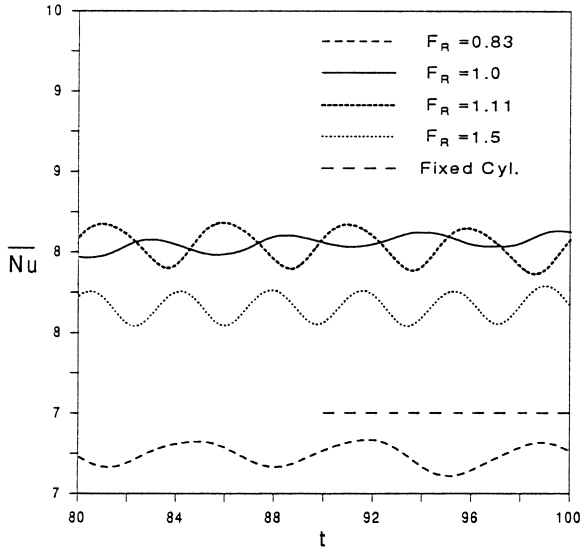

Fig. 9. The time variation of the average Nusselt number within the lock-on range of frequencies at $Re = 200$ and $\Theta_A = \pi/2$.

The isotherm patterns for a typical lock-on regime ($Re = 200$, $\Theta_A = \pi/2$) at the two frequency ratios, $F_R = 0.83$ and $F_R = 1.11$, are shown in Figs. 10 and 11, respectively. In both figures, the time period between plots is one quarter of a complete cycle. The shedding vortices appear in these figures as lumps of heated fluid being convected away from the cylinder. The locations of such vortices are exactly the same as appearing in equivorticity lines (not shown here). The number of these detached lumps of heated fluid in case of $F_R > 1$ is more than that in case of $F_R < 1$ indicating higher rate of vortex shedding and heat convection. Moreover, the mechanism of heat diffusion within each vortex as it moves downstream is clearly shown in these figures. For example, Fig. 11(b) shows that the fluid contained within each vortex gets cooler as it moves away from the cylinder (the number of isotherms indicate the temperature level). The periodicity of the thermal field in each case can be easily verified from the isotherm plots since the beginning of the cycle is very much the same as the end of it (see Fig. 10(a) and (e) and also Fig. 11(a) and (e)).

Fig. 12 shows the distribution of local Nusselt number within a complete cycle for the case of $Re = 200$, $\Theta_A = \pi/2$ and $F_R = 1.11$. The Nu distributions show that the maximum Nu values are almost the same. The locations of these maximums oscillate with the cylinder oscillation within a range of about $\pm 15^\circ$ around $\theta = 180^\circ$. It can be also observed that the Nu distribution at the middle of the cycle ($t = t_0 + 1/2\ T$) is a mirror image of that at the end of it ($t = t_0 + T$), which explains the asymmetry of the thermal field every half

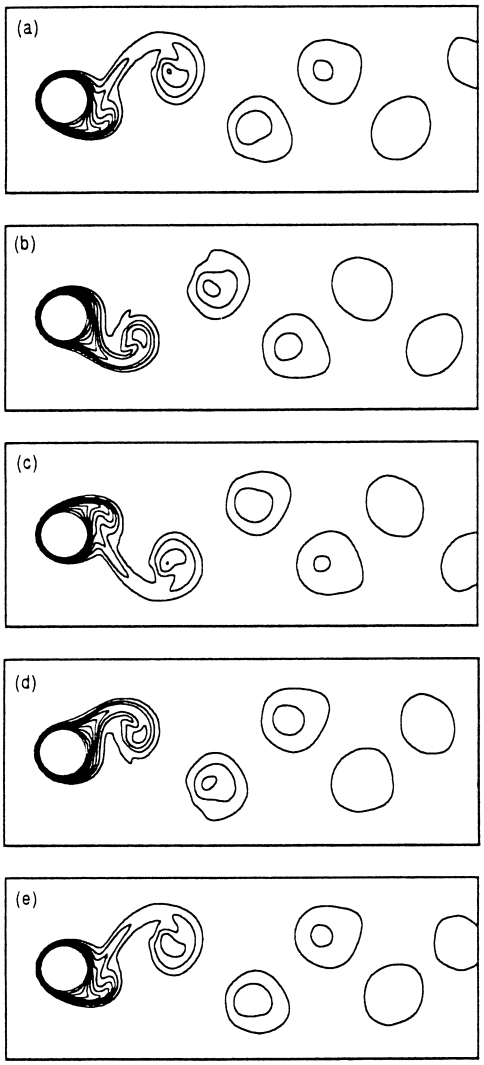

Fig. 10. Isotherm patterns for a complete cycle of lock-on regime at $Re = 200$, $\Theta_A = \pi/2$ and $F_R = 1.11$; (a) $t = t_0$, (b) $t = t_0 + 0.25\ T$, (c) $t = t_0 + 0.5\ T$, (d) $t = t_0 + 0.75\ T$, (e) $t = t_0 + T$, where T is the time period. The isotherms plotted are $\phi = 0.1(0.1)1.0$.

cycle. This phenomenon can be also ascertained by comparing the isotherm patterns shown in Fig. 10(a) and (c) and also Fig. 11(a) and (c). In comparison with Fig. 7, Fig. 12 shows that the Nu curve is flatter near its maximum which results in higher rate of heat transfer for this lock-on case. On the other hand, the fluctuations in Nu at any fixed location are more in the lock-on regime. For instance, at $\theta = 60^\circ$, the fluctuations in Nu reach 4.6 for lock-on regime, whereas it reaches 2.2 for the case of unlock-on regime. The computed time-averaged Nusselt number for the cases considered are presented in Table 2. The table also contains the percentage increase/decrease in heat trans-

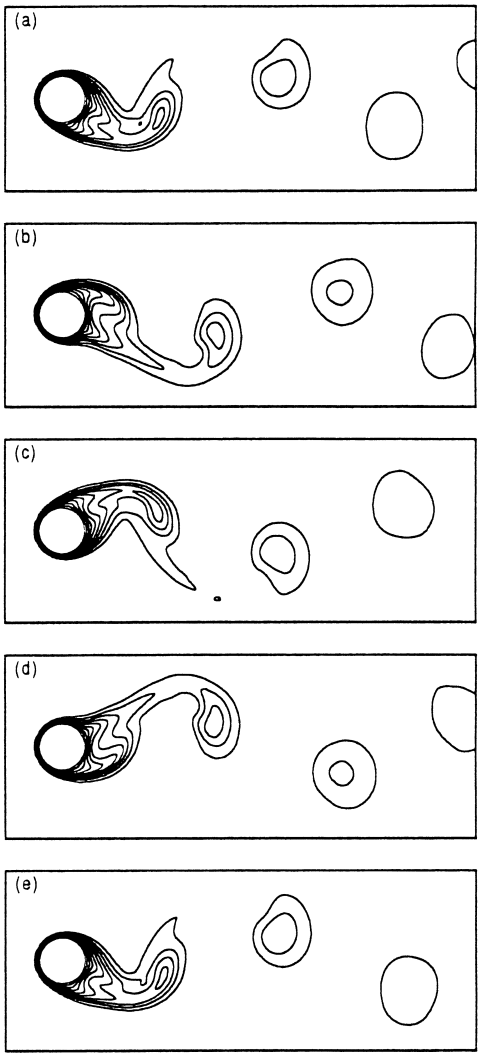

Fig. 11. Isotherm patterns for a complete cycle of lock-on regime at $Re = 200$, $\Theta_A = \pi/2$ and $F_R = 0.83$; (a) $t = t_0$, (b) $t = t_0 + 0.25T$, (c) $t = t_0 + 0.5T$, (d) $t = t_0 + 0.75T$, (e) $t = t_0 + T$, where T is the time period. The isotherms plotted are $\phi = 0.1(0.1)1.0$.

fer in comparison with the case of a fixed cylinder. The results show that a sensible enhancement in heat transfer is observed at $Re = 200$. One can also observe that this enhancement reaches its maximum near $F_R = 1$ for large amplitudes. At high frequencies outside the lock-on range, a slight enhancement in heat transfer is found at low amplitudes, however, as the amplitude increases, the enhancement in heat transfer decreases. For example, 8.7% increase in $\overline{\overline{Nu}}$ is found at $Re = 200$, $\Theta_A = \pi/8$ and $F_R = 2$. This percentage decreases to 5.8, 3.15 and 2.3 as the amplitude increases to $\Theta_A = \pi/4$, $\pi/2$ and π, respectively.

For better understanding of the response of heat transfer to changes in the amplitude and frequency of oscillations, let us consider the effect of each on the velocity and thermal fields. Larger amplitudes give rise to a larger shear layer wrapping the cylinder (or a good part of it) which tends to increase the momentum and thermal boundary-layer thicknesses leading to a reduction in Nu. On the other hand, as the frequency approaches the natural frequency, the fluid motion in the vicinity of the cylinder surface becomes more organized and intensive similar to what was found by Saxena and Laird [20]. The process of vortex shedding, though depends on amplitude and frequency, has a direct effect on heat convection since every vortex carries a certain amount of heat. The shedding frequency and the size of the vortices are both important factors influencing the heat convection process.

According to the obtained results, the amplitude of oscillation has an additional influence to the occurrence of the lock-on phenomenon. Larger amplitudes at frequencies near the natural frequency may create the lock-on phenomenon. Therefore, the effect of the amplitude is twofold; the first is the development of a larger shear layer and the second is the change of vortex shedding frequency. The two effects may have corroborating or contradicting effects on heat transfer depending on the frequency (whether greater than or less than the natural frequency). Within the lock-on range, lower frequency of vortex shedding results in less heat transfer. The effect of the rate of vortex shedding on heat transfer are indicated in Fig. 11. The figure shows that when $F_R > 1$ ($F_R = 1.11$ and 1.5), the heat transfer rate increases considerably in comparison

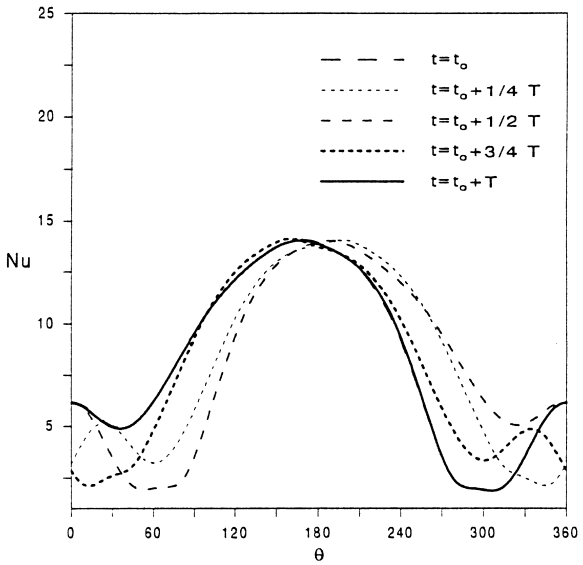

Fig. 12. The local Nusselt distribution in a complete cycle of lock-on regime at $Re = 200$, $\Theta_A = \pi/2$ and $F_R = 1.11$.

Table 2
Effect of amplitude and frequency of oscillations on the time-averaged Nusselt number

Re	Θ_A	F_R	$\overline{\overline{Nu}}$	$\overline{\overline{Nu}}$ ($F_R = 0$)	% Increase
		0.50	5.3		0
		0.75	5.4		1.8
100	$\pi/8$	1.00	5.4	5.3	1.8
		1.50	5.29		−0.19
		2.00	5.1		−3.7
		0.50	5.3		0
		0.75	5.16		−2
100	$\pi/4$	1.00	5.49	5.3	5.4
		2.00	5.31		0.1
		4.00	5.3		0
		0.50	5.25		−0.1
		0.75	5.25		−0.1
100	$\pi/2$	1.00	5.67	5.3	6.95
		1.50	5.43		2
		2.00	5.32		0.3
		0.50	7.28		4.1
		0.83	7.12		1.8
200	$\pi/8$	1.00	7.18	6.99	2.7
		1.50	7.34		5.0
		2.00	7.6		8.7
		0.50	7.35		5.10
		0.83	6.76		−3.30
200	$\pi/4$	1	7.01	6.99	2
		1.50	7.5		7.20
		2.00	7.4		5.80
		0.50	7.33		4.40
		0.83	6.73		−3.70
200	$\pi/2$	1.00	8.04	6.99	15.00
		1.50	7.66		9.50
		2.00	7.21		3.15
		0.50	6.97		−0.28
		0.83	6.5		−7.00
200	π	1.00	7.8	6.99	11.5
		1.5	7.42		6.10
		2	7.15		2.30

with that of a fixed cylinder. On the other hand, a decrease in $\overline{\overline{Nu}}$ may occur as the rate of vortex shedding decreases as observed in the case of low frequency lock-on regime ($F_R = 0.83$). The effect of synchronization is quite clear in Table 2 where the nearer the forcing frequency from $F_R = 1$, the higher the heat transfer. The reason for this increase may be attributed to the intensive fluid motion in the vicinity of the cylinder which leads to increase the rate of heat convection.

5. Conclusions

The problem of heat convection from a cylinder performing rotational oscillations in a cross stream is investigated in the range of Reynolds number, $Re \leq 200$, oscillation amplitude, $\Theta_A \leq \pi$ and frequency up to twice the natural shedding frequency. Similar to the velocity field, the thermal field in the wake region is influenced by the vortex shedding process. Such process has two distinct patterns; the first is the unlock-on pattern in which vortices are shed at the natural frequency and the second is the lock-on pattern in which vortex shedding is synchronized with the cylinder oscillations. The results revealed that the average Nusselt number fluctuates at twice the cylinder frequency with appreciable enhancement in heat transfer for high frequencies within the lock-on range. The effect of the amplitude is twofold; the first is the development of a larger shear layer, and the second is the change of vortex shedding frequency. The two effects may have corroborating or contradicting effects on heat transfer depending on the frequency (whether greater than or less than the natural frequency). Within the lock-on range, lower frequency of vortex shedding results in less heat transfer. The effect of oscillations on heat convection in the unlock-on regime is insignificant.

Acknowledgements

The authors wish to acknowledge the support received from King Fahd University of Petroleum and Minerals during this study. They also wish to thank the reviewers for their valuable comments that were instrumental in improving the manuscript.

References

[1] Y. Tanida, A. Okajima, Y. Watanabe, Stability of the circular cylinder oscillating in uniform flow or in a wake, J. Fluid Mechanics 61 (4) (1973) 769–784.
[2] R.E.D. Bishop, A.Y. Hassan, The lift and drag forces on a circular cylinder oscillating in a flowing fluid, Proceedings of the Royal Society, Series A (1964) 227.
[3] S.E. Hurlbut, M.L. Spaulding, F.M. White, Numerical Solution for laminar two dimensional flow about a cylinder oscillating in a uniform stream, ASME, J. Fluid Engineering 104 (1982) 214–222.
[4] P.K. Stansby, The locking-on vortex shedding due to cross-stream vibration of circular cylinder in uniform and shear flows, J. Fluid Mechanics 74 (1976) 641–665.
[5] O.M. Graffin, S.E. Ramberg, Vortex shedding from a cylinder vibrating in line with an incipient uniform flow, J. Fluid Mechanics 75 (1976) 257–271.
[6] A. Okajima, H. Takata, T. Asanuma, Viscous flow around a rotationally oscillating circular cylinder, Inst. Space and Aero. Sci. Rep. 532, University of Tokyo, 1975, pp. 311–337.
[7] P.T. Tokumaru, P.E. Dimotakis, Rotary oscillation control of cylinder wake, J. Fluid Mechanics 224 (1991) 77–90.

[8] X. Lu, J. Sato, A numerical study of flow past rotationally oscillating circular cylinder, J. Fluids and Structures 10 (1996) 829–849.
[9] M.H. Chou, Synchronization of vortex shedding from a cylinder under rotary oscillation, Computer and Fluids 26 (8) (1997) 755–774.
[10] E. Hori, Boundary layer on a circular cylinder in rotational oscillation, Bulletin of JSME 5 (17) (1962).
[11] S. Tanida, Visual observation of the flow past a circular cylinder performing a rotary oscillation, J. of the Physical Society of Japan 45 (3) (1978) 1038–1043.
[12] J.M. Wu, J.D. Mo, A.D. Vakili, On the wake of a circular cylinder with rotational oscillations, AIAA-89-1024, 1989.
[13] P.T. Tokumaru, P.E. Dimotakis, The lift of a cylinder executing rotary motions in a uniform flow, J. Fluid Mechanics 255 (1993) 1–10.
[14] J.R. Filler, P.L. Marston, W.C. Mih, Response of the shear layers separating from a circular cylinder to small-amplitude rotational oscillation, J. Fluid Mechanics 231 (1991) 481–499.
[15] B.G. Zijnen, Heat transfer from horizontal cylinder to a turbulent air flow, Applied Science Research A7 (1958) 205–223.
[16] C.T. Leung, N.W.M. Ko, K.H. Ma, Heat transfer from a vibrating cylinder, Journal of Sound and Vibration 75 (1981) 581–582.
[17] K. Takahashi, K. Endoh, A new correlation method for the effect of vibration on forced-convection heat transfer, Journal of Chemical Engineering, Japan 23 (1990) 45–50.
[18] S.P. Kezios, K.V. Prasanna, Effect of vibration on heat transfer from a cylinder in normal flow, Trans. ASME, Paper No. 66-WA/HT-43, 1966.
[19] K. Sreenivasan, A. Ramachandran, Effect of vibration on heat transfer from a horizontal cylinder to a normal air stream, Int. Journal of Heat and Mass Transfer 3 (1961) 60–67.
[20] U.C. Saxena, A.D.K. Laird, Heat transfer from a cylinder oscillating in a cross-flow, Trans. ASME, J. Heat transfer 100 (1978) 684–688.
[21] C. Chin-Hsiang, C. Horng-Nan, A. Win, Experimental study of the effect of transverse oscillation on convective heat transfer from a circular cylinder, Advances in Enhanced Heat Transfer, ASME HTD-Vol. 287 (1994) 25–43.
[22] D. Karanth, G.W. Rankin, K. Sridhar, A finite difference calculation of forced convective heat transfer from an oscillating cylinder, Int. Journal of Heat and Mass Transfer 37 (11) (1994) 1619–1630.
[23] C.-H. Cheng, J.L. Hong, A. Win, Numerical prediction of lock-on effect on convective heat transfer from a transversely oscillating circular cylinder, Int. J. Heat and Mass Transfer 40 (8) (1997) 1825–1834.
[24] E.P. Childs, R.E. Mayle, Heat transfer on a rotationally oscillating cylinder in cross-flow, Int. J. Heat and Mass Transfer 27 (1) (1984) 85–94.
[25] W.M. Collins, S.C.R. Dennis, Flow past an impulsively started circular cylinder, J. Fluid Mechanics 60 (1973) 105–127.
[26] H.M. Badr, S.C.R. Dennis, Time-dependent viscous flow past an impulsively started rotating and translating circular cylinder, J. Fluid Mech 158 (1985) 447–488.
[27] A. Roshko, On the development of turbulent wakes from vortex streets, NACA Rep., 1191, 1954.
[28] C.H.K. Williamson, Oblique and parallel modes of vortex shedding in the wake of circular cylinder at low Reynolds numbers, J. Fluid Mechanics 206 (1989) 579–627.
[29] E.R.G. Eckert, E. Soehngen, Distribution of heat transfer coefficients around circular cylinders in cross-flow at Reynolds numbers from 20 to 500, Trans. ASME 74 (3) (1952) 343–347.
[30] H.A. Kramers, Heat transfer from sphere to flowing media, Physics 12 (1946) p61.
[31] P.D. Richardson, Heat and mass transfer in turbulent separated flows, Chem. Eng. Sci 18 (1963) 149–155.
[32] V.T. Morgan, The overall convective heat transfer from smooth circular cylinder, in: J.P. Hartnett, T.F. Irvine Jr (Eds.), Advances in Heat Transfer, vol. 11, Academic Press, New York, 1975, pp. 199–264.
[33] P.C. Jain, B.S. Goel, A numerical study of unsteady laminar forced convection from a circular cylinder, J. Heat Transfer, Ser. C 98 (2) (1976) 303–307.
[34] A.A. Rashid, Steady-state numerical solution of the Navier–Stokes and energy equations around a horizontal cylinder at moderate Reynolds numbers from 100 to 500, Heat Transfer Engineering 17 (1) (1996) 31–81.